Biorheology 46 (2009) 309–321
DOI 10.3233/BIR-2009-0542
IOS Press

Dynamics of ballistically injected latex particles in living human endothelial cells

Yixuan Li *, Siva A. Vanapalli and Michel H.G. Duits
Physics of Complex Fluids, Department of Science & Technology, MESA+ Institute of Nanotechnology, University of Twente, Enschede, The Netherlands

Received 23 March 2009
Accepted in revised form 27 May 2009

Abstract. We studied the dynamics of ballistically injected latex particles (BIP) inside endothelial cells, using video particle tracking to measure the mean squared displacement (MSD) as a function of lag time. The MSD shows a plateau at short times and a linear behavior at longer times, indicating that the BIP are trapped into a viscoelastic network. To reveal more about the molecular constituents and the dynamics of this actin network, we added a variety of drugs. Latrunculin and Jasplakinolide aimed at intervening with the actin network caused a strong increase in MSD, whereas Taxol aimed at microtubules gave no measurable change in MSD. Additional corroborating information about these drug effects were obtained from MSD amplitude and exponent distributions and from fluorescent staining images of the actin and microtubule networks. Our evidence strongly suggests that BIP are primarily embedded in the actin network. Additional drug interventions aimed at disabling non-thermal forces could not conclusively resolve the nature of the forces driving BIP dynamics.

Keywords: Endothelial cells, actin cytoskeleton, viscoelasticity, ballistic injection, particle tracking

1. Introduction

The use of video microscopy to study the statistical motions of colloidal particles inside living cells (intracellular particle tracking), has potential to become one of the future methods for diagnosis of individual cells. There are several reasons for this: (1) the dynamics of intracellular particles is sensitive to the mechanical state of a cell, which in turn depends on its health condition [13,15,20]; (2) colloidal particles are easily visualized, and their size is ideally suited to probe the cytoskeleton's mechanics [35]; (3) since low power light sources can be used, the measurements are in principle non-invasive; (4) because many intracellular particles are available [6,34] or can be introduced [27], and representative responses can be obtained for individual cells, and (5) combination of microscopy and microfluidics should allow for parallel or high throughput analysis of cells in chips [9,26]. However the complex architecture and dynamics of the living cell also creates a major obstacle: without deeper insight into the origins of the intracellular particle motions, only an empirical knowledge is generated about the relation between the measured mean squared displacements (MSD) of the particles and the state of the cell, to cite one example. While this can be valuable for distinguishing between healthy and diseased cells, it

*Address for correspondence: Yixuan Li, Physics of Complex Fluids, Department of Science & Technology, University of Twente, Postbus 217, 7500 AE Enschede, The Netherlands. Tel.: +31 53 489 3097; Fax: +31 53 489 1096; E-mail: Y.Li@tnw.utwente.nl.

contributes little to achieving generic insights. In contrast, if intracellular particle dynamics could be linked more systematically to physical quantities (such as rheological properties) or the behavior of specific cytoskeletal structures (such as the dynamics of the actin network), then a more conceptual picture would be obtained and a comparison between different measurements might be possible. For externally enforced global deformations of the cell, successes were recently achieved through the use of either AFM [7] or optical stretching [11] to measure the apparent elastic modulus of the cell. Intracellular particle tracking appears to have a similar potential [28,33].

Developments in the field thus call for fundamental studies into the origins of erratic intracellular particle motions. From the literature [13,19,30–32], it becomes clear that a measured MSD depends on: (1a) in what kind of micro environment (ME) the particles inhabit; (1b) how the particles interact with this ME, and (1c) what drives the motions of the particles. These three questions are obviously related to each other, and often the answers are at least partially unknown.

The ability to address any of these sub-questions can already be valuable. For example, the annihilation of non-thermal (ATP dependent) driving forces through chemical intervention could allow use of the fluctuation–dissipation theorem as done in microrheology [22]. In that case, intracellular rheological properties such as the visco-elasticity of the cytoskeleton could be obtained. Encouraging results along this line were obtained by Hoffman et al. [13] where a universality in particle dynamics was found after ATP depletion. Also, knowledge of the physico-chemical interactions between a particle and its ME could simplify interpretation. For example, probes with a binding affinity for specific intracellular components (such as microtubules or the actin network) could be used as sensors for the fluctuations of these networks. Paradoxically, achieving such simplifying conditions requires insight into the complexity of the cell. Additional questions which then arise are: (2) can probes with a similar surface chemistry be assumed to occur in comparable micro environments?, and (3) can non-thermal driving forces indeed be eliminated, or alternatively, revealed?

This paper reports on an attempt to address questions (1)–(3). We present experiments on human endothelial cells, for which we found a rather different dynamics for Endogenous Granules (EG), as described in another paper [34], than for microinjected latex particles in the present paper. Our carboxylated poly(styrene) latex particles have also been studied in previous particle tracking and microrheology studies, because of their negative surface charge and low binding affinity to actin [24,30,31]. Moreover, there is no evidence that these particles are 'recognized' by the cell and hence undergo important changes (like encapsulation) at relevant experimental timescales. However, in what local ME these particles occur has not been systematically studied, and whether or not motions of these particles in these cells are driven by ATP-dependent processes or not (at typical timescales for video particle tracking), has not been demonstrated either.

To reveal the microenvironment of the BIP (question (1)), we exposed our cells to a variety of drugs that specifically interfere with either the actin network or microtubules. We also attempted to shed more light on the role of ATP-dependent processes, by depleting the intracellular ATP and by adding Blebbistatin, whose primary effect is to disable actomyosin contractility. Besides MSD averaged within cells (and over different cells), we also studied variations in the dynamics displayed by different BIP in the same cell. This allowed us to also address the questions (2) and (3), through study of histograms for the MSD amplitude and exponent.

This paper is organized as follows: in Section 2 we will discuss all experimental aspects of cell culture, drug treatments, staining, ballistic particle injection, microscopy and particle tracking. The analysis of mean squared displacements is discussed in Section 3. In Section 4 we present the effect of drugs on

ensemble averaged MSD, on the distributions of the individual MSD and on cytoskeletal structure as visualized by staining. In Section 5, conclusions are drawn.

2. Materials and methods

2.1. Cell culture

Human microvascular endothelial cells (Hmec-1) at 25–30 passages, were cultured at 37°C in a humidified 5% CO_2 environment in endothelial cell growth medium containing hydrocortisone, hFGF, R3-IGF-1, ascorbic acid, hEGF, gentamicin, heparin, and 2% fetal bovine serum (EGM-2, Lonza, Basel, Switzerland). For our microscope experiments, cells were plated on a Delta T culture dish (Bioptechs, Butler, PA, USA), that had been coated for 1 hour with fibronectin (100 µg/ml solution). A heated lid was used to prevent solvent evaporation losses, and cells were maintained at 37°C and 5% CO_2 during tracking experiments. Cultures were typically at 50% confluence, which allowed studying individual cells. Under these conditions, and before drug treatment, most of our cells showed morphologies such as those illustrated in Fig. 1(A). Also different morphologies (e.g. cells undergoing division) were sometimes encountered. These cells were excluded from the analysis, to minimize contamination of the results.

2.2. Probe types

In this study we mainly worked with ballistically injected particles (BIP). For these, we chose monodisperse, red-fluorescent carboxylated poly(styrene) latex particles with diameter 0.2 µm (Invitrogen) and excitation/emission wavelength 565/610 nm. These probes appear as bright spots in confocal fluorescent mode (Fig. 1(A)). For comparative purposes, we also studied some cells with endogenous granules (EG). These granules, which appear as dark objects under phase contrast microscopy (Fig. 1(A)), were confirmed to be mainly lipid droplets after staining with Nile Red (Invitrogen). The mean size of the granules was assessed to be ∼0.5 µm. Unless mentioned otherwise, BIP and EG were studied in separate cells.

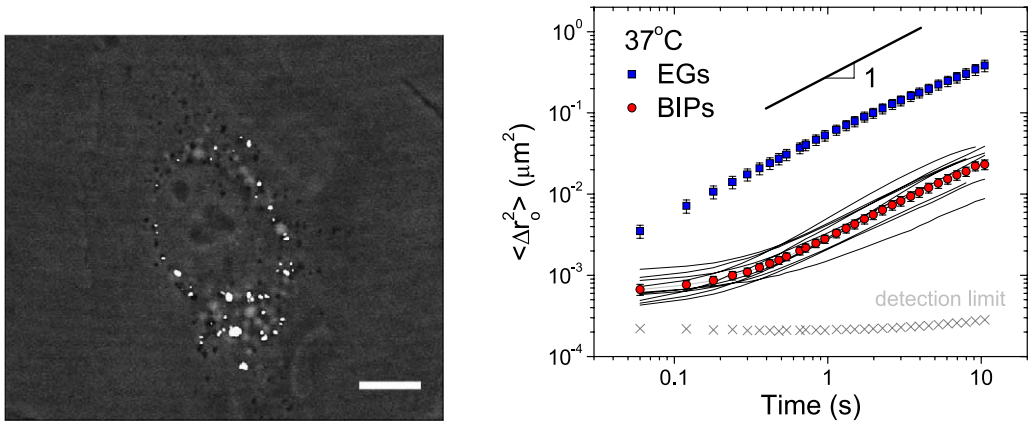

(A) (B)

Fig. 1. (A) Illustration of the cellular distributions of BIP (bright spots) and EG (dark spots) in a single Hmec-1 cell. Scale bar is 10 µm. (B) Mean Square Displacement versus lagtime functions for EG (squares) and BIP (circles) in cells under physiological conditions. Results are averaged over 10 cells, and error bars indicate the standard deviation of the mean. For BIP also the results for the individual cells are shown. Cross symbols show a measurement of the (BIP) latex particles glued onto a coverslip.

2.3. Ballistic injection

Ballistic injections of tracer particles were carried out using a Biolistic gun (Bio-rad) and a procedure similar to that described in Panorchan et al. [21,27] (but without hepta adapter). Using optimized injection parameters (vacuum level 28 mmHg, Helium pressure 1350 psi, carrier disk-to-sample distance 3 cm), we achieved a $\sim$50% survival rate of the cells. After bombardment, a recovery time of 30 min was allowed before trypsinizing and replating the cells. Of the surviving cells, only those that contained 15–40 particles were selected for tracking experiments. Sometimes aggregates of BIP were observed; these were excluded from the analysis.

2.4. Drug interventions on cytoskeleton and myosin motors

All drugs were purchased from Sigma Aldrich, except Blebbistatin (Tebu-bio, Belgium). The following interventions were done: Latrunculin A (200 nM, incubation time 2 h), Jasplakinolide (25 μM, 1 h), Nocodazole (5 μM, 3 h), Cephalomannine (Taxol, 100 μM, 1 h), Blebbistatin (50 μM, 2 h). 2-D-deoxyglucose and Sodium Azide at final concentrations of 50 mM and 0.05% respectively were applied for 30 min as an ATP-depletion cocktail. Each drug intervention effect was measured by 2–5 independent experiments, i.e. adding freshly prepared drug solution to fresh cells. A typical tracking experiment lasted 2–3 hours after the end of drug incubation.

2.5. Immunofluorescence microscopy

To stain the intracellular structures, cells were rinsed with phosphate buffer saline (PBS) solution and fixed with 4% formaldehyde in PBS at 37°C for 8 min. Next, cells were permeabilized with a PBS solution containing 0.2% Triton-X and 0.1% BSA (Sigma-Aldrich). FITC-phalloidin (1 μM) was used to stain F-actin. For microtubule staining, mouse anti-α-tubulin antibody (1 mg/l) was applied for 20 min, after which the sample was thoroughly washed with PBS and further immersed in a solution of Rhodamine conjugated goat anti-mouse antibody (1 mg/l) for 20 min. Immuno-fluorescence was viewed using our confocal microscope described below. Stainings were performed immediately after the incubation time.

2.6. Multiple particle tracking

Probe particles were visualized using the UltraView LCI10 system (Perkin Elmer), in which a Yokogawa spinning-disk confocal unit is combined with a Nikon Eclipse TE-300 inverted microscope. A 100$\times$ (NA 1.3) oil immersion objective was used. BIP were visualized in confocal fluorescence mode (using the 564 nm Kr line), while endogenous granules were imaged in phase contrast mode. Approximately 2500 images were recorded with a (Hamamatsu) 12-bit CCD camera at $\sim$17 frames per second for a typical duration of 150 seconds. The spatial resolution corresponding to the images was 0.13 μm per pixel. In each cell, 50–100 EG and 15–40 BIP were tracked. The particles were identified using the publicly available particle-tracking code [14] based on [5], written and extended in Interactive Data Language (IDL) by several authors. The localization error was measured to be $\sim$15 nm (Fig. 1(B)) by measuring the MSD of probe particles attached to a coverslip. For each experimental condition (i.e. drug treatment), 10 different cells were studied, giving 10^3–(5×10^3) trajectories (larger than the total number of particles, due to repeated displacements in and out of the focal plane).

2.7. Data analysis

Our data analysis, more extensively described in [8] is based on the particle tracking rheology method as demonstrated by Gittes et al. and Mason et al. [10,23] and first applied to living cells in 2002 by Tseng et al. [30]. Besides the usual Mean Squared Displacement $\langle \Delta r^2 \rangle(\tau)$, obtained by averaging over displacements of the same particle as well as over the different particles present in the cell, we also examined individual particle MSDs (iMSDs). Both MSDs and iMSDs were analyzed by fitting a power law to their local behavior around a chosen lagtime τ_0:

$$\langle \Delta r^2 \rangle \approx A(\tau/t_0)^{\alpha},$$

where A is the amplitude, τ the lagtime and t_0 the unit exposure time (60 ms). A and α provide complementary information on the respective displacement magnitude and the type of the motion (from sub to super-diffusive). The iMSD were analyzed at different lagtimes τ_0, producing an amplitude $A(\tau_0)$ and exponent $\alpha(\tau_0)$. Histograms for these quantities were obtained by averaging over the different cells under the same experimental condition (i.e. drug treatment). These distributions are compared with reference curves for a viscous liquid and an elastic solid in Section 4.

3. Results

3.1. Ensemble dynamics of BIP

As a reference case we first consider the cells without interventions (other than the injection with BIP). The typical morphology of a single Hmec-1 cell is shown in Fig. 1(A), which also illustrates how the BIP are spread over the intracellular space. Figure 1(B) shows the MSD obtained by averaging over 10 different Hmec-1 cells, along with the results for the individual cells. As will be shown, these differences between cells are modest compared to the effects caused by the interventions. Two characteristic regions can be found in the MSD-time curve: (i) for short lag times ($<$0.3 s), the onset of a plateau is found, indicative of an elastic environment, and (ii) for $\tau > 1.0$ s a nearly diffusive behavior is found, evidenced by a powerlaw exponent α of 0.92 ± 0.02.

At this point it is also interesting to compare the dynamics of BIP to that of the endogenous granules studied in the same cells earlier by us [34]. The MSD taken from the latter study are included in Fig. 1(B). Remarkably, for EG the amplitude is almost an order of magnitude higher than for BIP, although the (typical) radius of the EG is 2.5 times larger. In addition, the EG do not display a quasi-plateau region in the MSD at short times, but an apparently diffusive behavior for the entire time range.

To corroborate this result, we performed an additional experiment in which both probes were tracked inside the very same cell. Here, the plot of all individual MSD was found to correspond well to combined plots of iMSD from EG and BIP measured in separate cells (not shown). In addition we verified that the different dynamics of the two probes is not due to obvious differences in intracellular location. Making a distinction between perinuclear and perimembrane areas for 10 different Hmec-1 cells, we found that 91% of the BIP were found in the perinuclear area, while it was 86% for the EG. These observations confirm the fact that the strong (qualitative and quantitative) differences in dynamics between EG and BIP in Hmec-1 cells are due to the occurrence of these probes in entirely different local microenvironments.

3.2. Interpretative approach

As also pointed out in other particle tracking studies in cells (e.g. [32]), the complexity of the analysis of intracellular MSD necessitates a certain interpretative approach. MSD measurements cannot provide specific clues unless combined with additional information. *A priori*, our MSD data could reflect mechanical properties of the actin network (AN), microtubules (MT), or the cytoskeleton as a whole. Also *a priori*, thermal collisions or ATP driven processes or a combination thereof could be responsible for the mechanical excitations (especially in the time range of 0.1–30 s as addressed by our experiments, see [25]). Hence we will discuss differences or changes in MSD magnitude only in the context of a competition between driving forces (tending to increase the amplitude) and resistance (to be called "stiffness") offered by the visco-elastic network (tending to reduce the amplitude).

To explore changes in driving force or stiffness, we added a variety of drugs aimed at selectively interfering with either the actin network or the microtubules. Since interpretation can be confounded by secondary effects (responses by the cell) we explored two different drugs per cytoskeleton component. Also drugs aimed at eliminating ATP-dependent driving mechanisms were explored. Images of cells stained for actin and tubulin were assumed to qualitatively represent cytoskeletal changes.

3.3. Drug interventions aimed at the actin network

3.3.1. Latrunculin A

In an attempt to break down the F-actin network, Latrunculin A (LA) was applied at a concentration of 0.2 μM during 2 hours (similar conditions as in [13]) before the particle tracking experiments were started. The averaged MSD (top curve in Fig. 2) shows that the elastic plateau for $\tau < 0.3$ s has largely disappeared, and that the slope of the MSD curve has become close to 1.0 over a large time range. An increase in MSD might be expected when the stiffness of the particle's micro environment is reduced while the driving forces are kept intact. The occurrence of a power law exponent of 1.0 over two decades could suggest that the viscoelastic cytoplasm had transformed into a viscous liquid. This issue will be further addressed in Section 3.5.

The disappearance of the elastic region at $\tau < 0.3$ s in LA-treated cells turned out to be highly reproducible. Shorter exposures to LA were also explored, where the effect on MSD was less pronounced

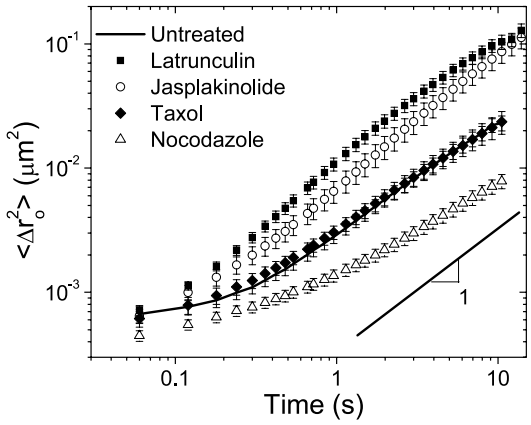

Fig. 2. Effects of various cytoskeletal interventions on BIP dynamics. MSD of untreated BIP (–), after exposure to latrunculin A (■), jasplakinolide (○), taxol (♦), nocodazole (Δ).

(data not shown). As a control, we also performed a cell recovery test by replacing LA treated culture medium with the normal culture medium. Two hours after the LA had been removed, a significant number of the cells exhibited MSD in which the elastic plateau had been fully restored. This suggests that the intervention with LA is reversible. More importantly, it shows that the change in the BIP dynamics was not related to a change in cell status (for example, apoptosis) but due to the depletion of the actin network.

The effect on LA on the actin cytoskeleton was corroborated by the microscopy images. In line with the observations in [32], the cell morphology was found to have changed into a typical 'balled-up' shape. Our fluorescent staining images showed that the stress fibers had completely disappeared. Only discrete actin aggregates at the peri-membrane area were still visible (see Fig. 3H).

3.3.2. Jasplakinolide

Jasplakinolide is known for its specific interference with the (de-)polymerization of actin, and has also been used in studies of the actin cytoskeleton. However its stabilizing effect on the actin network *in vitro* [3] does not necessarily transfer to a similar effect *in vivo*, as evidenced by a study in which Jasplakinolide was found to *disrupt* the actin network inside cells [4]. After exposing our Hmec-1 cells to 25 μM Jasplakinolide for 1 h followed by fluorescent staining, we found that the actin appeared depleted in the perinuclear area, but also that actin stress fibers still persisted in the peri-membrane area (see Fig. 3(C and I)). Interestingly, this suggests that mechanical methods that mostly probe the cell membrane, such as Magnetic Twisting Cytometry or (low amplitude) Atomic Force Microscopy, could measure a different effect of Jasplakinolide than the intracellular techniques such as our PTR method.

In our experiment, the depletion of actin in the perinuclear area (where most of our particles are found) again caused an increase in the MSD amplitude and powerlaw exponent. This is in line with expectations based on the LA intervention experiment. Apparently the effect of Jasplakinolide is slightly less strong compared to that of LA.

3.4. Drug interventions aimed at microtubules

3.4.1. Taxol

Taxol has been widely explored for its ability to stabilize MT [29,37]. It inhibits the depolymerization of MT and hence changes the balance between MT growth and catastrophe. The consequence is that many short MT units are formed. Indeed, our fluorescent staining images (Fig. 3(E and K)), revealed that after treatment with 100 μM for 1 h, the majority of MT had become fragmented (or highly curved). In contrast, no changes in the actin network were visible. The effect of taxol intervention on the averaged MSD of BIP turned out to be negligible, which is remarkable for such a drastic intervention. The simplest explanation for this is that, neither the driving force nor the stiffness of the micro-environment for the BIP is changed. Additional support for this argument will be provided in Section 3.5.

3.4.2. Nocodazole

Nocodazole interferes in a rather different way with MT than does taxol. It can bind to the β-subunit of tubulin and promote depolymerization of MT. As a result, the MT are destroyed, which can also lead to changes in the cell shape. On longer time scales ($>$12 h) Nocodazole interferes with the cell cycle, synchronizing cells to the G2/M state. To minimize this effect, we used a high dosage (5 μM) of Nocodazole during a short time (3 hours). As claimed in [36], this treatment should not increase cell death or change the actin or intermediate filament cytoarchitecture. The fluorescent staining images in Fig. 3 (D and J) confirm the expected disappearance of the MT network, whereas the actin network appears to

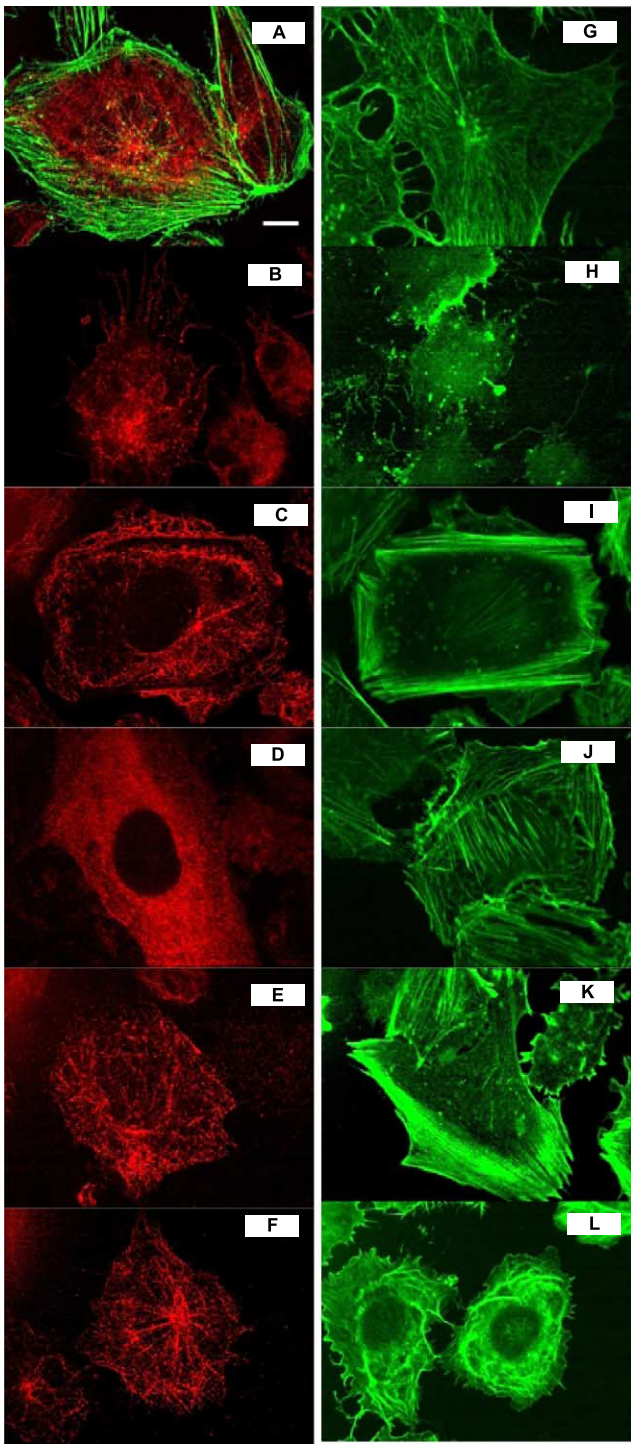

Fig. 3. Fluorescent staining images of actin (green) and microtubules (red) in Hmec-1 cells before (A) and after treatments with drugs (B–L). G – ATP depletion (actin only); B, H – latrunculin A; C, I – jasplakinolide; D, J – nocodazole; E, K – taxol; F, L – blebbistatin. Scale bar is 10 μm. (The colors are visible in the online version of the article.)

be unaffected. The amplitude and power-law exponent of the MSD show a significant reduction due to Nocodazole treatment, implying a reduction in driving force and/or a stiffening of the micro-environment of the BIP.

3.5. Individual dynamics of BIP

To further study the effects of the drug interventions, we now turn to the analysis of (the statistics of) individual trajectories. First we consider Fig. 4(A and B), which show typical trajectories for BIP inside two different Hmec-1 cells. As with other cells [30], here it is also observed that a considerable spread exists amongst the trajectories of different particles inside the same cell.

We analyzed this heterogeneity by fitting local power laws (Section 2.7) to individual MSD functions and then grouping the results for different cells at the same condition into the same histogram. To allow objective comparison between different experiments [8] we segmented all trajectories into blocks of 200 steps before calculating the iMSDs. Fitting the local amplitude (A) and exponent (α) around $\tau \approx 0.1$ s, produces the histograms in Fig. 5(A and B). Fitting around $\tau \approx 1.0$ s produces Fig. 5(C).

First we remark that all curves in Fig. 5 show broadening due to the finite number (i.e. 200) of steps per (segmented) trajectory. This is clearly illustrated by the dotted curves marked with SL (simple liquid), which represent a measurement of particles with radius $a = 100$ nm in a water/glycerol mixture with viscosity $\eta \approx 100$ mPa s at $T = 298$ K. In such a liquid, all particles have the same expectation value for the amplitude ($A = 2\tau kT/3\pi\eta a$) and exponent ($\alpha = 1.0$). However, due to the limited statistics, a measurement inaccuracy is superimposed [8]. To illustrate this further, we also present a distribution of α measured for an elastic gelatin gel (GG) (10 wt% in water at 24°C) in Fig. 5(B). Since this curve is centered around $\alpha \approx 0$, the statistical broadening (or measurement error) now gives rise to negative values. Also the occurrence of negative exponents down to ~ -0.15 for the BIP in Fig. 5(B) should be seen in this light.

In spite of the broadening, several interesting observations can still be made from Fig. 5. First of all it is clear that BIP under physiological conditions do not display a simple behavior. At lagtimes $\tau < 0.3$ s where a plateau-like MSD was found, both the amplitude and the exponent display a broad distribution. The tail in Fig. 5(B) is at least partly due to a few diffusive trajectories, as are illustrated in Fig. 4(B). We recall that all histograms in Fig. 5 are averages over multiple (typically 10) cells. Making up the

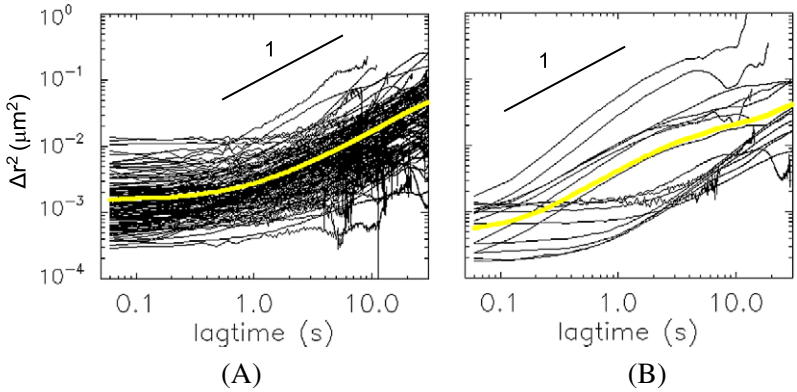

Fig. 4. Overview of individual MSD (black) and total MSD (light grey) for two selected Hmec-1 cells loaded with BIP. (A) Shows the transition from a plateau to a diffusive behavior in the overall MSD; (b) shows how both elastic-like and diffusive-like behaviors can occur at small lagtimes in the same cell.

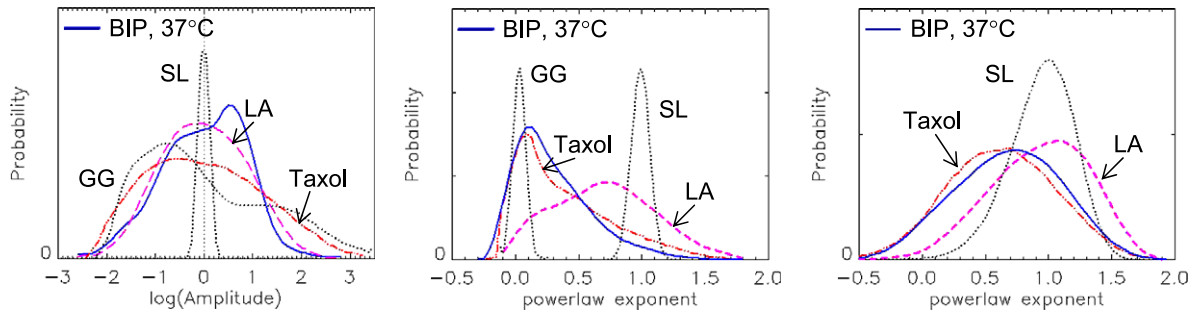

Fig. 5. Probability distributions for the (normalized) amplitude of the iMSD at ∼0.1 s (A), and its local exponent at ∼0.1 s (B) and ∼1.0 s (C). In (A) all amplitudes have been divided by the average over 10 cells at the same condition. Solid lines: BIP in Hmec-1 cells at 37°C. Dashed-dotted curves: after Taxol treatment. Dashed curves: after treatment with Latrunculin A (LA). For comparison, also reference curves for particles in a simple liquid (SL) and a gelatin gel (GG) are given. In (A) and (B) these have been multiplied with 0.2 and 0.4 respectively.

histograms for individual cells, the distributions were found slightly narrower but still considerably broader than the SL distribution (data not shown).

Secondly we discuss the effect of administering LA and Taxol on the histograms for BIP in Fig. 5. These two interventions are especially interesting in view of their dramatically different effects on the average MSD of EG [8] and BIP (Fig. 2). For BIP, LA was found to give an average MSD that suggested simple diffusive behavior. But as seen from Fig. 5, it results in fact in a more complex behavior. The distribution for α now reveals superdiffusive contributions (both at 0.1 and at 1.0 s), since the fraction with $\alpha > 1.0$ is clearly larger than that of the SL curve. This suggests that at least after the treatment with LA, non-thermal driving forces are acting on BIP. Possibly, these forces also acted in the absence of LA (but then without manifesting themselves via the distribution of α). In contrast, exposing the cells to Taxol has an almost negligible effect on the exponent distribution. This indicates that it is rather unlikely that the active motions of MT are driving the dynamics of BIP (even if this happened indirectly e.g. as with MT bending fluctuations shaking the actin network [2]).

Finally we note from Fig. 5(A) that the amplitude distribution is broad for all systems except SL. The curve for LA once more corroborates that the dynamics after intervention with LA is not simply diffusive. This could suggest that there is still an intact network that is capable of modulating the motions of the BIP. Interestingly, even the curve for gelatin (rheologically speaking, a simple elastic solid) shows a large amplitude heterogeneity (we have no tentative explanation for the detailed shape of this distribution). The amplitude heterogeneity for both the cytoskeleton and gelatin gels could point to a distribution in local stiffness, e.g. due to variations in the density of elastic strands. Alternatively it could also indicate a heterogeneity in probe-matrix contacts, as previously suggested [32]. This is an interesting issue, which merits further study.

3.6. Drug interventions aimed at disabling active processes

3.6.1. ATP depletion

Inspired by the results of [13] we also attempted to switch off the non-thermal driving forces by depleting ATP. Unlike previous studies with EG [2,34] in which strong amplitude reductions were observed, we found a twofold increase in the MSD-time curve for our BIP, without any change in the shape of the curve. Also the histograms for A and α did not significantly change due to the ATP depletion (results

not shown). This counterintuitive increase in average MSD implies that there were secondary effects. We attribute these to a decrease in the stiffness, possibly caused by a weakening of the actin network. A partial depletion of this network is suggested by the images of the stained cells (Fig. 3G).

3.6.2. Blebbistatin

Since this drug specifically inhibits the action of myosin II isoforms, by preventing reattachment of the myosin head after the power stroke [18], its effect could provide a clue as to the importance of actomyosin contractility. At the level of MSD we found that the amplitude was reduced by a factor 2, while the exponent α at $\tau \approx 1$ s had decreased to 0.7 ± 0.1 (not shown). However, we also found that the morphology of the cells had changed (see Fig. 3(F and L)): the cells had shrunk, peripheral stress fibers had been lost, and accumulation of clumps of actin had appeared in cytoplasm. This indicates that not only the primary effect on the myosin motors but also secondary effects like a stiffening of the cytoskeleton may have contributed to the change in MSD.

4. Discussion

4.1. Micro-environment of the BIP in the living cytoskeleton

Most of our observations give positive indications that our injected carboxylated latex particles are embedded in the actin network. The interventions with Latrunculin and Jasplakinolide provide strong supporting evidence – breaking down the AN (in the perinuclear region where almost all particles reside) gives rise to a disappearance of the elastic plateau, and increased motion amplitudes. The shape of the MSD (time) curves for the BIP can then be explained from the transient nature of the AN. Since our BIP are bigger than the reported mesh size for intracellular F-actin (50 nm in [30], 100 nm in [12]), they should become trapped in the cages provided by the actin network. However since the AN is a dynamic entity (modulated by a number of proteins that crosslink, bundle, sever and cap actin filaments [1]) the cages will have a certain life-time. Beyond this timescale, the BIP will explore the AN at much larger length scales, resulting in a different, more diffusive-like dynamics.

Our observations do not indicate a strong link between the dynamics of BIP and the microtubules. Already, evidence against such a link came from our previous study [34], where it was concluded that EG are intimately connected to MT. Together with the enormous difference in MSD amplitude for EG and BIP, this excludes the possibility that also the BIP are linked to microtubule networks. The difference in microenvironment for BIP and EG becomes even more apparent when comparing the effects of drugs. Taxol, which had a strong effect on the MSD of EG, did not produce a significant change in the dynamics of BIP, while Latrunculin that dramatically altered the MSD of BIP, did not significantly affect the MSD of EG. The only observation which does not directly fit with our hypothesis that BIP are embedded in the actin network is the Nocodazole intervention, which needs to be addressed in the future.

4.2. Driving forces for BIP

Based on our observations we are unable to draw hard conclusions about the mechanism(s) that drive the motions of BIP. The much lower motion amplitudes compared to EG, seem to rule out that BIP are likewise driven by bending fluctuation of the MT. The insensitivity of the MSD of BIP to the Taxol intervention also suggests that indirect excitation, in which the AN transmits the MT fluctuations to the BIP, is unlikely.

Our results could still be consistent with acto-myosin contractility (AMC) as a driving force. The superdiffusive behavior observed after the LA intervention could in principle be due to AM driven contractions of the remaining actin network. And to the extent that the effect of Blebbistatin can be ascribed to the annihilation of AMC, the decrease in MSD could be explained by a loss of AMC. Finally, the effect of Nocodazole could also be seen in the light of the reported increase in actomyosin contraction force [16,17].

However as already stated in Section 3.2, the complexity of the cellular response can also obscure the relation between the primary effect of a drug and the change in MSD. Hence, additional evidence will be needed to resolve the question concerning driving forces.

5. Conclusions and outlook

Successful injection of many particles per cell allowed us to perform a systematic study of the dynamics of BIP in Hmec-1 cells. The signature of the MSD of BIP was entirely different than that earlier found for EG. Drug interventions indicated that (unlike EG, which occur close to microtubules), BIP are predominantly embedded in the actin network. This network behaves qualitatively as a viscoelastic liquid, with cage trapping at short lag times and more diffusive-like behavior at longer times. The mechanism by which the BIP are driven could not be conclusively revealed from the present work.

The fact that intracellular particle MSD are very sensitive to drug-induced changes in the state of the cell, confirms the potential for eventually using intracellular PTR in clinical studies. Moreover, since BIP and EG are associated with specific cytoskeletal biopolymer networks, they could form a dual probe system for both applied and fundamental research into cellular mechanical behavior.

Acknowledgements

We are grateful to Frieder Mugele for discussions, and to Denis Wirtz and Liesbeth Pierson for advice on ballistic particle injection. We thank Andries van der Meer and André Poot for providing cell lines and cell culture training. This research was supported by the Cell Stress program of the MESA$^+$ Institute of Nanotechnology.

References

[1] B. Alberts, A. Johnson, J. Lewis, M. Raff et al., *Molecular Biology of the Cell*, Garland Science, New York, 2002.
[2] C.P. Brangwynne, F.C. MacKintosh and D.A. Weitz, Force fluctuations and polymerization dynamics of intracellular microtubules, *PNAS USA* **104** (2007), 16128–16133.
[3] M.R. Bubb, A.M.J. Senderowicz, K.L.K. Duncan and E.D. Korn, Jasplakinolide, a cytotoxic natural product, induces actin polymerization and competitively inhibits the binding of phalloidin to F-actin, *J. Biol. Chem.* **269** (1994), 14869–14871.
[4] M.R. Bubb, I. Spector, B.B. Beyer and K.M. Fosen, Effects of Jasplakinolide on the kinetics of actin polymerization: an explanation for certain *in vivo* observations, *J. Biol. Chem.* **275** (2000), 5163–5170.
[5] J.C. Crocker and D.G. Grier, Methods of digital video microscopy for colloidal studies, *J. Coll. Interface Sci.* **179** (1996), 298–310.
[6] J.C. Crocker and B.D. Hoffman, Multiple-particle tracking and two-point microrheology in cells, *Methods Cell Biol.* **83** (2007), 141–178.
[7] S.E. Cross, Y.S. Jin, J. Rao and J.K. Gimzewski, Nanomechanical analysis of cells from cancer patients, *Nat. Nanotechnol.* **2** (2007), 780–783.
[8] M.H.G. Duits, Y. Li, S.A. Vanapalli and F. Mugele, Mapping of spatiotemporal heterogeneous particle dynamics in living cells, *Phys. Rev. E* **79** (2009), 051910.

[9] J. El-Ali, P.K. Sorger and K.F. Jensen, Cells on chips, *Nature* **442** (2006), 403–411.
[10] F. Gittes, B. Schnurr, P.D. Olmsted, F.C. MacKintosh and C.F. Schmidt, Microscopic viscoelasticity: Shear moduli of soft materials determined from thermal fluctuations, *Phys. Rev. Lett.* **79** (1997), 3286–3289.
[11] J. Guck, S. Schinkinger, B. Lincoln, F. Wottawah et al., Optical deformability as an inherent cell marker for testing malignant transformation and metastatic competence, *Biophys. J.* **88** (2005), 3689–3698.
[12] W. Gutkowski and T.A. Kowalewski (eds), Mechanics of the 21st Century, in: *Proceedings of the 21st International Congress of Theoretical and Applied Mechanics*, Warsaw, Poland, 15–21 August, 2004, Springer, 2005.
[13] B.D. Hoffman, G. Massiera, K.M.V. Citters and J.C. Crocker, The consensus mechanics of cultured mammalian cells, *PNAS USA* **103** (2006), 10259–10264.
[14] http://www.physics.emory.edu/∼weeks.idl/.
[15] D.E. Ingber, Mechanobiology and diseases of mechanotransduction, *Ann. Med.* **35** (2003), 564–577.
[16] M.S. Kolodney and E.L. Elson, Correlation of myosin light chain phosphorylation with isometric contraction of fibroblasts, *J. Biol. Chem.* **268** (1993), 23850–23855.
[17] M.S. Kolodney and E.L. Elson, Contraction due to microtubule disruption is associated with increased phosphorylation of myosin regulatory light chain, *PNAS USA* **92** (1995), 10252–10256.
[18] M. Kovacs, J. Toth, C. Hetenyi, A.M. Csizmadia and J.R. Sellers, Mechanism of Blebbistatin inhibition of myosin II, *J. Biol. Chem.* **279** (2004), 35557–35563.
[19] A. Lau, B.D. Hoffman, A. Davies, J.C. Crocker and T.C. Lubensky, Microrheology, stress fluctuations, and active behavior of living cells, *Phys. Rev. Lett.* **91** (2003), 198101.
[20] G.Y.H. Lee and C.T. Lim, Biomechanics approaches to studying human diseases, *Trends Biotechnol.* **25** (2007), 111–118.
[21] J.S. Lee, P. Panorchan, C.M. Hale, S.B. Khatau et al., Ballistic intracellular nanorheology reveals ROCK-hard cytoplasmic stiffening response to fluid flow, *J. Cell Sci.* **119** (2006), 1760–1768.
[22] T.G. Mason, Estimating the viscoelastic moduli of complex fluids using the generalized Stokes–Einstein equation, *Rheol. Acta* **39** (2000), 371–378.
[23] T.G. Mason, K. Ganesan, J.H.V. Zanten, D. Wirtz and S.C. Kuo, Particle tracking microrheology of complex fluids, *Phys. Rev. Lett.* **79** (1997), 3282–3285.
[24] J.L. McGrath, J.H. Hartwig and S.C. Kuo, The mechanics of F-actin microenvironments depend on the chemistry of probing surfaces, *Biophys. J.* **79** (2000), 3258–3266.
[25] D. Mizuno, C. Tardin, C.F. Schmidt and F.C. MacKintosh, Nonequilibrium mechanics of active cytoskeletal networks, *Science* **315** (2007), 370–373.
[26] A.L. Paguirigan and D.J. Beebe, Microfluidics meet cell biology: bridging the gap by validation and application of microscale techniques for cell biological assays, *Bioessays* **30** (2008), 811–821.
[27] P. Panorchan, J.S. Lee, B.R. Daniels, T.P. Kole et al., Probing cellular mechanical responses to stimuli using ballistic intracellular nanorheology, *Methods Cell Biol.* **83** (2006), 115–140.
[28] P. Panorchan, J.S. Lee, T.P. Kole, Y. Tseng and D. Wirtz, Microrheology and ROCK. Signaling of human endothelial cells embedded in a 3D matrix, *Biophys. J.* **91** (2006), 3499–3507.
[29] P.B. Schiff and S.B. Horwitz, Taxol stabilizes microtubules in mouse fibroblast cells, *PNAS USA* **77** (1980), 1561–1565.
[30] Y. Tseng, T.P. Kole and D. Wirtz, Micromechanical mapping of live cells by multiple-particle-tracking microrheology, *Biophys. J.* **83** (2002), 3162–3176.
[31] M.T. Valentine, Z.E. Perlman, M.L. Gardel, J.H. Shin et al., Colloid surface chemistry critically affects multiple particle tracking measurements of biomaterials, *Biophys. J.* **86** (2004), 4004–4014.
[32] K.M. Van Citters, B.D. Hoffman, G. Massiera and J.C. Crocker, The role of F-actin and myosin in epithelial cell rheology, *Biophys. J.* **91** (2006), 3946–3956.
[33] S.A. Vanapalli, M.H.G. Duits and F. Mugele, Microfluidics as a functional tool for cell mechanics, *Biomicrofluidics* **3** (2009), 012006.
[34] S.A. Vanapalli, Y. Li, F. Mugele and M.H.G. Duits, On the origins of the universal dynamics of endogenous granules in mammalian cells, *Mol. Cell. Biomech.* **150** (2009), 1–16.
[35] D. Weihs, T.G. Mason and M.A. Teitell, Bio-microrheology: A frontier in microrheology, *Biophys. J.* **91** (2006), 4296–4305.
[36] D. Weihs, T.G. Mason and M.A. Teitell, Effects of cytoskeletal disruption on transport, structure and rheology within mammalian cells, *Phys. Fluids* **19** (2007), 1031021–1031026.
[37] A.C. Yvon, P. Wadsworth and M.A. Jordan, Taxol suppresses dynamics of individual microtubules in living human tumor cells, *Mol. Biol. Cell* **10** (1999), 947–959.